A NEW ERROR RESILIENCE TECHNIQUE USING ADAPTIVE FMO AND INTRA REFRESH IN H.264 VIDEO CODING

Vu Huu Tien(*), Supavadee Aramvith(**), Yoshikazu Myanaga(***)
(*) Posts and Telecommunications Institute of Technology, Vietnam
(**) Chulalongkorn University, Bangkok, Thailand
(***) Hokkaido University, Sapporo, Japan

(Bài đăng trên tạp chí **"IEICE The Institute of Electronics, Information and Communication Engineers"** – Nhật Bản, số 8, quyển E94-A, xuất bản ngày 1/8/2011)

Abstract: *In this paper, we proposed an error resilience scheme for wireless video coding based on adaptive Flexible Macroblock Ordering (FMO) and intra refresh. An FMO explicit map is generated frame-by-frame using prior information. This information involves estimated locations of guard and burst section in the channel and estimated effect of error propagation (EEP) from the previous frame to the current frame. In addition, the role of the current frame in propagating an error to the next frame is also considered. A suitable intra refresh rate which is adaptive to channel state is used to reduce the dependency between frames and thus can stop the EEP. The results in experiments show that our proposed method gains some improvements in terms of PSNR as compared to some other methods that have not considered channel condition and error propagation in generating FMO map.*

1. INTRODUCTION

As a new tool of H.264/AVC, Flexible Macroblock Ordering (FMO) enables an image to be divided into regions called slice groups. Each slice group can be divided in several slices and a slice can also be decoded independently. An identification number for each Macroblock (MB) is given by a MacroBlock Allocation map (MBAmap) to specify which slice group that MB belongs to. The number of slice groups is limited to 8 for each picture to prevent complex allocation schemes. A suitable MBAmap disperses important MBs in to some slice groups. Because of independency between slice groups, if a slice group is in error, the important MBs in the other slice groups are not affected.

To design slice group maps, previous approaches use an indicator to evaluate the importance of an MB. The indicator is determined as bitcount [2], distortion-from-error concealment [3], MB impact factor [4] or Spatial Temporal Indicator [5]. After that, MB's are sorted in descending order of importance and arranged consequently to 8 slice groups. As another approach to generate FMO map, MBs first are dispersed into two slice groups and the splits them further into more slice groups according to the impact factor of MBs [6]. By dispersing important MBs, the number of lost MBs is reduced. However, important MBs are not protected from error thoroughly. Because of variable length coding, if an MB is in error, the following important MBs in the same slice group are also affected. Therefore, using only FMO is not enough to reduce the number of lost important MBs. In [3], channel state is considered to combine with FMO. If channel state is bad, FMO and interleaving is used. In [7], redundant slices are added depending on the characteristic of wireless channel. In this method, ROI slices are transmitted in a good state of the channel. In bad state, redundant slices are transmitted. Nevertheless even in the good state, there may be some errors in the channel. Thus, important MBs in a good state may still be affected by error. In addition, by adding redundant slices, compression efficiency of video codec is reduced.

When transmitting video signal over error-prone channels like wireless channels, beside error caused by the transmission channel, error propagation between frames is a problem that must be taken into account. To stop error propagation, intra refresh algorithm is used. However, the selecting of a suitable intra refresh rate is a problem that needs to be considered. Intra MBs can effectively stop error propagation, but the number of intra MBs in a frame is limited by compression efficiency. Coding efficiency will be reduced if the intra refresh rate is high because of rate-distortion optimization. Moreover, with limited target bit rate allocated for each frame, a frame with high number of intra MBs consumes a high target bit and thus affects to the target bit of the next frames. Thus, it is necessary to balance the benefit of reducing error propagation effect and the drawback of using a high number of intra coded MBs in a frame.

Currently, there have been some systems focusing on computing optimized intra refresh rate. In [8], a fixed number of MBs with the highest distortion in the current frame are coded in intra mode. Another methods in [9], [10] choose the suitable MBs for intra coding by computing cost for each type of coding mode. However, the algorithm has to try all possible intra and inter modes and thus may cause delay in real-time applications.

In this paper, the effect of error propagation (EEP) which is estimated at each MB of the current frame is used as an indicator to generate a FMO map. In addition, by using three-state Markov model [11], [12], average burst length (ABL) and average guard length (AGL) of channel are computed. Based on ABL and AGL, the positions of burst and guard sections in the current frame are estimated. The MBs with low EEP are arranged in slice groups transmitted in burst sections. The MBs with high EEP belong to slice groups which are transmitted in guard section. Within a section, MBs are dispersed to some slice groups. Furthermore, a suitable number of MBs with highest importance in guard sections are selected for coding in intra mode.

Three-state Markov model and channel conditions are introduced in Section 2. Section 3 proposes the method to generate a FMO explicit map. Section 4 shows the simulation results and discussions. Finally, conclusions are given on Section 5.

2. LOCATING BURSE AND GUARD SECTIONS OVER WIRELESS CHANNELS

2.1. Three – State Markov Model [11, 12].

In this section, three-state Markov model in [11] and [12] is introduced. However, instead of the model in bit level [11], [12], we apply three-state Markov model in packet level to estimate the position of error bursts over a wireless channel.

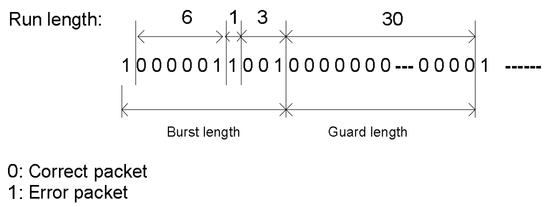

Fig.1 Packet sequence for an error channel

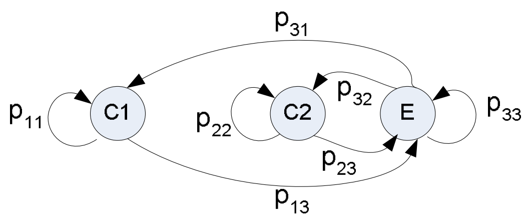

Fig.2 Three-state Markov Model.

Fig.1 shows an example of the packet sequence in an error channel. Similarly to [11], [12], we define the following definitions at packet level. A guard section is defined as an error-free section and a burst section is defined as the section sandwiched between guard sections. The minimum guard length is the minimum length of error free packets. In this work, the minimum guard length of 30 packets is used as a result from empirical studies. Thus, each guard section is longer than 30 consecutive error-free packets. The run length is defined as a length from an error packet to the next error packet excluding the first error packet. The first return probability P(i) is defined as the occurrence probability of each run length i and the cumulative first return probability is obtained as the cumulation of the first return probability.

Fig. 2 shows the transition probabilities of a three-state Markov model where C_1 and C_2 show error-free states which are state 1 and state 2, and E shows the error state which is state 3. C_1 shows a guard section while C_2 and E show a burst section. P_{nm} is probability of transition from state n to state m. The p_{nn}^{i-2} is the probability of the case in which there are *(i-2)* consecutive transitions from state n to state n. The first return probabilities are computed as

$$\begin{aligned} P(1) &= prob(E/E) = p_{33} \\ P(2) &= prob(C_1, E/E) + prob(C_2, E/E) \\ &= p_{31}p_{13} + p_{32}p_{23} \\ &\cdots \\ P(i) &= prob(C_1,...,C_1, E/E) + prob(C_2,...,C_2, E/E) \\ &= p_{31}p_{11}^{i-2}p_{13} + p_{32}p_{22}^{i-2}p_{23} \end{aligned} \quad (1)$$

where $prob(\alpha/\beta)$ means that β is the first state and then the sequence of α occurs.

The transition probabilities are computed in (2),

$$\begin{aligned} p_{33} &= P(1) \\ p_{32} &= \sum_{i=2}^{L} P(i) \\ p_{23} &= \frac{p_{32}}{\sum_{i=2}^{L_{\min}} (i-1)P(i)} \\ p_{31} &= 1 - p_{33} - p_{32} \\ p_{13} &= 1 \Big/ \left(\sum_{i=L_{\min}+1}^{\infty} (i-1)P(i)/p_{31} - L_{\min} \right) \\ p_{22} &= 1 - p_{23} \\ p_{11} &= 1 - p_{13} \end{aligned} \quad (2)$$

where L_{min} is the minimum guard length. The *average guard length,* L_G, and *average burst length,* L_B, are computed as

$$\begin{aligned} L_G &= L_{\min} + \frac{1}{p_{13}} \\ L_B &= \frac{\frac{p_{31}}{p_{13}} + \frac{p_{32}}{p_{23}} + 1}{p_{31}p_{11}^{L-1}} - \left(1 + \frac{1}{p_{13}}\right) \end{aligned} \quad (3)$$

2.2. Locating Error Burst Positions

Assume that before encoding the current frame *(n)*, an encoder receives the feedback information containing the position of error packets of the previous frame *(n-2)*. From the information, the encoder uses (3) to compute values L_G and L_B of the channel. These values are used for the whole transmission duration of current frame *(n)* and a previous frame *(n-1)*. Then values of L_G and L_B are updated when encoder receives the next feedback information. To estimate burst section or guard section, the position of the last burst or guard section of the past frames are used. If the border of frame *(n-2)* and frame *(n-1)* is in a guard section (see Fig. 3), the distance from the last burst in the past frames to the first burst in frame *(n-1)* is L_G packets. Otherwise, if the border is in a burst section, the distance from the last guard in the past frames to the first guard in frame *(n-1)* is L_B packets. The next sections in frame *(n-1)* and frame *(n)* are estimated from the position of the first section.

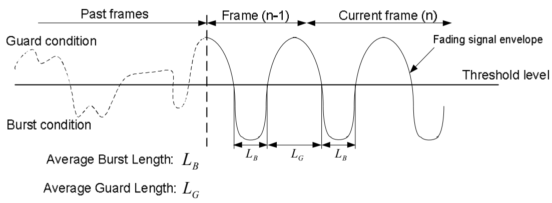

Fig.3 Estimation of AGL and ABL for the current frame

Fig. 4 and 5 illustrate the estimation of error burst locations for 100 frames of Akiyo sequence in fast and slow fading. The average length of each P frame in this video sequence is 27 packets. The first I frame of video sequence has 430 packets. The estimation starts from the fourth frame of video sequences. The (a) of figures shows the estimation of the locations of burst and guard sections. The (b) shows the actual locations of burst and guard in the error pattern. The (c) shows differences between estimation and reality. The results show the estimation in slow fading case is more precise than that in fast fading case.

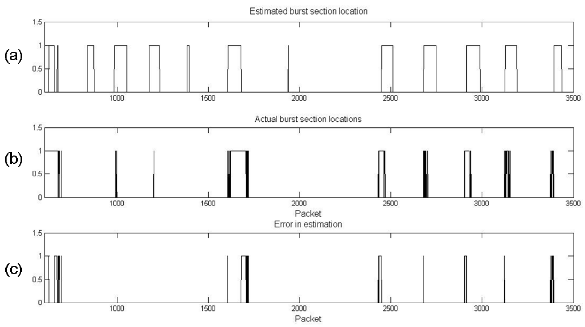

Fig.4 Akiyo sequence in slow fading case.
(a) Estimated locations of burst and guard
(b) Actual location of burst and guard
(c) Differences between estimated and actual locations

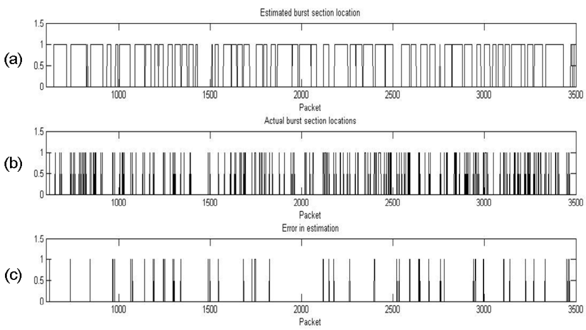

Fig.5 Akiyo sequence in fast fading case.
(a) Estimated locations of burst and guard
(b) Actual location of burst and guard
(c) Differences between estimated and actual locations

3. ADAPTIVE EXPLICIT FMO MAP GENERATION

Based on the bitcount in the first pass of MBs, AGL and ABL from (3), we will arrange MBs to slice groups with the condition that the high important MBs will be put in guard sections of channel and the low important MBs will be put in the burst sections (Fig. 6).

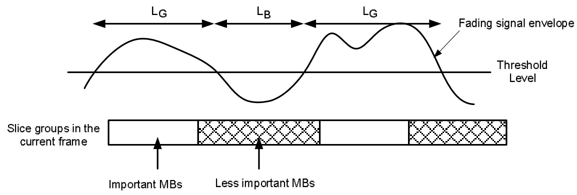

Fig.6 Arranging MBs into slice groups in the current frame

3.1. Effect of Error Propagation Estimation

As mentioned above, to make decision intra or inter coding mode for an MB in the current frame, firstly, we estimate the distortion at the MB caused by error MBs in the previous frame. Secondly, we measure the effect of error propagation from this MB to the next frame when it is coded in inter mode. If the distortion is high and the effect of the error propagation in the next frame is large, the considered MB will be selected for intra coding mode. Fig. 7 describes the error propagation from the previous frame to the current frame and to the next frame. We estimate the distortion at each pixel in the current frame *(n)* caused by error propagation from the error pixel in frame *(n-2)*. Then distortion, which propagated from each pixel of frame *(n)* to frame *(n+1)*, is measured. The sum of distortions caused by frame *(n-2)* to frame *(n)* and by frame *(n)* to frame *(n+1)* at each MB in the current frame is taken into account for generating explicit FMO map and for inter/intra coding mode decision.

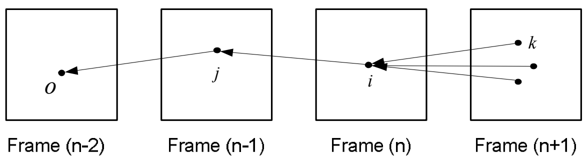

Fig.7 Error propagation from the previous frame to the next frame

Step 1: Compute the distortion caused by the error pixel in frame *(n-2)* to frame *(n-1)*:

Assume that a pixel *j* in a frame *(n-1)* refers to a pixel *o* in frame *(n-2)*. If the pixel *o* in frame *(n-2)* is error, the decoder will copy the pixel *o* of frame *(n-3)* since the non-motion compensated error concealment method is used. Therefore distortion at pixel *j* in frame *(n-1)* is computed as shown in (4),

$$D(j,n-1)=\begin{cases}\big\|f(j,n-1)-f(o,n-2)\big|- & \text{the pixel } j\in \text{inter coded pixels}\\ -\big|f(j,n-1)-f(o,n-3)\big\| & \\ 0 & \text{the pixel } j\in \text{intra coded pixels}\end{cases} \tag{4}$$

where *f(x,y)* is reconstructed value of the pixel x^{th} in the frame y^{th}.

If the pixel *o* in the frame *(n-2)* is error free, the distortion at pixel *j* in frame *(n-1)* is computed in (5).

$$D(j,n-1)=0 \tag{5}$$

Step 2: Compute EEP from frame *(n-1)* to frame *(n)*:

Assume that the pixel *i* in the frame *(n)* refers to the pixel *j* in the frame *(n-1)*. The value *p* is error probability of MB containing the pixel *j*. If the pixel *j* is inter coded, the distortion at the pixel *i* is computed as

$$D(i,n)=\begin{cases}p\big\|f(j,n)-f(j,n-1)\big|- & \text{the pixel } j \text{ is error}\\ -\big|f(i,n)-f(j,n-2)\big\| & \\ (1-p)D(j,n-1) & \text{the pixel } j \text{ is error free}\end{cases} \tag{6}$$

In this case, the distortion at the pixel *i* is computed as shown in (7)

$$D(i,n-1)=p\big\|f(i,n)-f(j,n-1)\big|-\big|f(i,n)-f(j,n-2)\big\|+ \\ +(1-p)D(j,n-1) \tag{7}$$

If the pixel *j* is intra coded, the distortion at the pixel *i* is computed as

$$D(i,n)=\begin{cases}p\big\|f(i,n)-f(j,n-1)\big|- & \text{the pixel } j \text{ is error}\\ -\big|f(i,n)-f(j,n-2)\big\| & \\ 0 & \text{the pixel } j \text{ is error free}\end{cases} \tag{8}$$

In this case, the distortion at pixel *i* is computed as shown in (9).

$$D(i,n)=p\big\|f(i,n)-f(j,n-1)\big|-\big|f(i,n)-f(j,n-2)\big\| \tag{9}$$

Step 3: Compute EEP from frame *(n)* to frame *(n+1)*: To compute EEP from the previous frame to the next through the current frame, all MBs in the current frame are coded in inter mode in the first pass. Assume that pixel *i* in the current frame is referred by a pixel *k* in the next frame. The distortion caused by error propagation at pixel *k* is computed as shown in (10),

$$D(k,n+1)=\begin{cases}q\big\|f(k,n+1)-f(i,n)\big|- & \text{the pixel i is error}\\ -\big|f(k,n+1)-f(i,n-1)\big\| & \\ (1-q)D(i,n) & \text{the pixel i is error free}\end{cases} \tag{10}$$

where *q* is error probability of the pixel *i*. The overall distortion propagated from the pixel *i* in the current frame *(n)* to the next frame *(n+1)* is computed as shown in (11),

$$I(i,n)=\sum_{m\in\{N\}}D(m,n+1) \tag{11}$$

where *N* is the number of pixels in the frame *(n+1)* which refer to the pixel *i* in the current frame *(n)*.

Step 4: Estimate the total distortion of an MB in the current frame:

From (9) and (11), the total distortion of the l^{th} MB in the current frame is computed as

$$D_{MB}(l,n)=\sum_{i=1}^{256}\left[D(i,n)+I(i,n)\right] \quad (12)$$

3.2. Adaptive Explicit FMO Map

In this work, two-pass architecture is used for encoding. In the first pass, all MBs in the P frame are encoded in inter mode. Note that in this pass, encoded frames are not transmitted to decoder. The purpose of the first pass is to know motion vector and packet number of MBs. In the second pass, after getting feedback information from the past frame, L_G and L_B are computed and the positions of burst and guard sections are predicted for the current frame. Based on the total distortion computed in (12), MBs are selected to fill in each section until the total packet number of selected MBs equals to the length of section.

The number of slice groups in a section, N_{slg}, is computed as shown in (13),

$$N_{s\lg}=\left\lfloor\frac{H}{13}\right\rfloor+1 \quad (13)$$

where $\lfloor z\rfloor$ means the largest integer which is not greater than z. H is the number of MBs selected to fill in the current section. In the guard section, some MBs with highest overall distortion are selected for intra coding mode. The number of intra MBs in the guard section, N_{Intra}, is computed as shown in (14).

$$N_{Intra}=\gamma N_{s\lg} \quad (14)$$

To balance the compression efficiency and effect of error propagation, γ is empirically selected to 2. According to (14), an intra refresh rate depends on the number of guard sections, thus the number of intra MBs in frames can be varied from 0 (if there is no guard section in transmission duration of frame) to 16 (if the whole frame is transmitted within a guard section). In addition, since intra coded MBs are dispersed in some slice groups in guard sections, the intra MBs are higher guaranteed than in the case without knowing about guard and burst locations. Flow chart of algorithm for arranging MB is shown in Fig. 8.

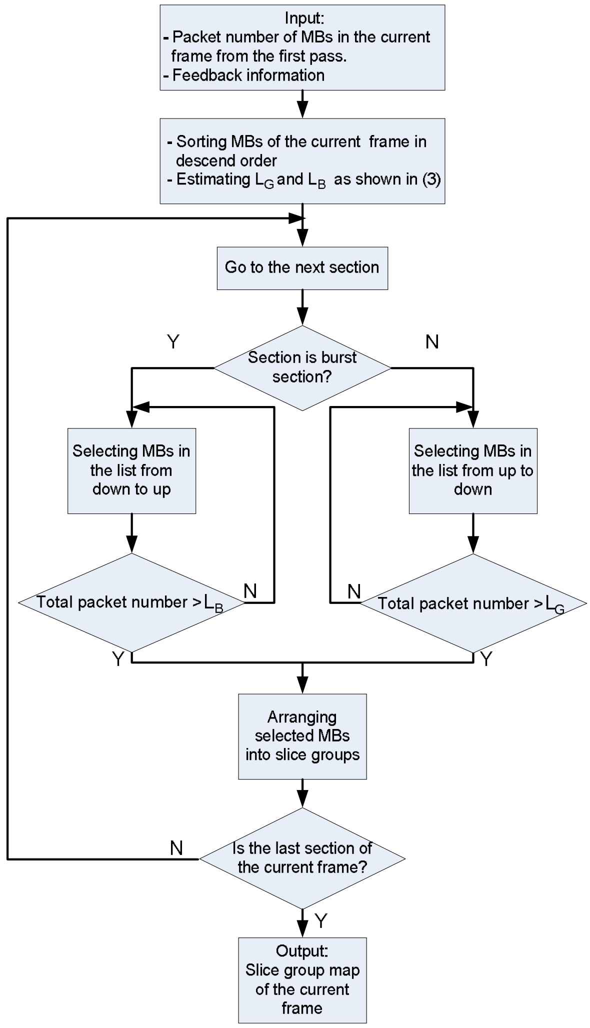

Fig.8 Flow chart of proposed method

3.3. Conditions in Experiments

To analyze the effectiveness of using the proposed explicit FMO map for video transmission in comparison with the previous works, the reference software JM 9.2 is used. Baseline profile is used at the encoder. At the decoder, the non-motion compensated error concealment is used. The following video sequences are used in experiment: Akiyo, Foreman, Carphone and Claire. Each sequence is encoded for a total of 100 frames at a frame rate of 10 f/s. Rate control is enabled and bit rate is set at 32kbps. The default encoder parameters are used with the exception of FMO and related parameters. See [13] for detailed information about the

H.264 JM encoder parameters. To investigate the benefits of using FMO on wireless channel, the Rayleigh fading wireless channel simulator is used in this simulation. The details of the simulator can be found in [14]. To simulate the effects of slow and fast fading channels, the maximum Doppler frequency parameter is set to 1Hz, for slow fading and 40Hz, for fast fading [14].

4. RESULTS AND ANALYSIS

In this experiment, to evaluate the efficiency of using EEP as an indicator for FMO as well as the correctness of channel prediction method, the proposed method is compared to some other methods using different indicators, including bitcount [2] and Spatial-Temporal Indicator [5]. Further more, to validate the method of selecting MBs for intra coding mode and computing intra refresh rate, the proposed method is compared to methods using Fix number of Intra MB (FI) [7] and Random Intra Refresh (RIR) [15]. In comparisons, PSNR is used as the performance metric in quantifying the effectiveness of methods.

Table 1 shows the average PSNR of video sequences in the scenario of slow and fast fading channels. The simulation results show that the proposed method without intra refresh and channel prediction (no IR + no CP) gains higher average PSNR than the previous methods. Especially, if compared to the method of no using FMO, the improvement of average PSNR is up to 5 dB. However, in some cases, PSNR of the new method is lower. This is because the quality of measurements of video in term of PSNR depends solely on the location of bit errors and also the error concealment method applied. In this experiment, simple non-motion compensated error concealment is used. Results show that the average PSNR is improved when channel prediction is applied to the proposed method. This is because the number of lost important MBs is reduced when the locations of burst and guard sections are estimated. However, in the fast fading case, the improvement is not much higher compared to the case without channel prediction. The reason is the channel prediction algorithm is more precise in slow fading case. In fast fading case, there are more errors in the position estimation of burst and guard sections. Therefore, the number of lost important MBs in fast fading case is higher than that in slow fading case. Consequently, in fast fading case, the effectiveness of channel estimation is not as high as in slow fading case.

Table 1 Comparison of Average PSNR (dB)

PSNR (dB)	Akiyo		Foreman		Claire		Carphone	
	Slow	Fast	Slow	Fast	Slow	Fast	Slow	Fast
No FMO	30.22	26.59	17.67	15.54	28.37	24.65	22.41	19.75
Bit count	34.62	32.14	21.28	18.32	32.14	28.87	25.34	22.95
STI-FMO	33.75	30.7	21.56	18.37	32.20	28.94	25.55	22.45
Proposed method (no IR + no CP)	34.29	31.29	**21.8**	**19.5**	**33.19**	28.8	**25.98**	**24.41**
Proposed method (no IR + CP)	**35.02**	**32.71**	**23.82**	18.4	**33.9**	**30.45**	**27.58**	**24.61**

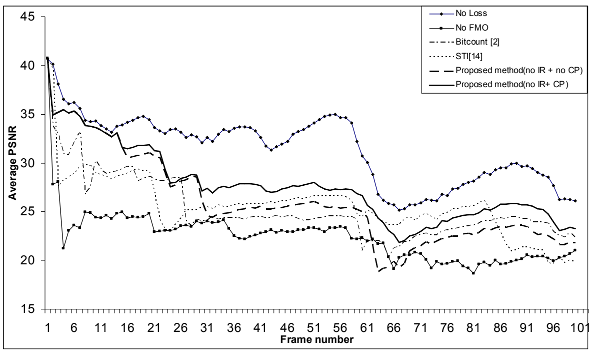

Fig. 9 PSNR comparison of Carphone in Slow fading

Fig. 9 and Fig. 10 show PSNR curve of Carphone test sequence in the slow and fast fading case, respectively. From the curves, it can be observed that the average PSNR of the proposed method is higher than the others. This improvement is achieved by using an accurate method in stopping the effect of error propagation. In addition, by estimating locations of burst and guard sections, important MBs are put in error-free sections, thus the number of lost important MBs is reduced. Consequently, the PSNR of the new method is increased.

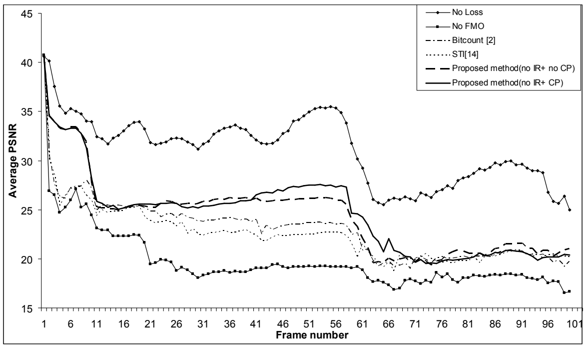

Fig. 10 PSNR comparison of Carphone in Fast fading

Table 2 Comparison of Average PSNR (dB)

PSNR (dB)	Akiyo		Foreman		Claire		Carphone	
	Slow	Fast	Slow	Fast	Slow	Fast	Slow	Fast
Random IR[12]	34.39	30.09	21.77	20.61	31.47	27.61	25.04	22.25
Fixed IR [6]	34.36	30.05	21.29	17.5	33.59	30.69	26.42	24.53
Proposed method (Fixed IR + no CP)	34.05	31.85	22.49	19.16	32.6	30.78	27.39	23.87
Proposed method (Adaptive IR+CP)	34.58	33.13	24.83	19.9	33.08	31.63	28.39	26.15

Table 2 shows average PSNR of video sequences when comparing proposed method using adaptive intra refresh rate with other methods using fix and random intra refresh rate. In the first scene, the proposed method uses the fix intra refresh rate without channel prediction. The results show that with considering effect of error propagation from the current frame to the next frame, the proposed method has average PSNR higher than that of method used in [8] (bold results). In both of methods, the fix number of intra refresh rate is 11 MBs [8]. In [8], only errors propagated from the previous frame to the current frame are taken into account. Consequently, some error MBs in the current frame are skipped in considering coding mode because these MBs may not be much affected by error propagation. However, these MBs may have much effectiveness to the next frame. Therefore, it is necessary to consider both effect of error propagation from the previous frame to the current frame and from the current frame to the next frame. In the second scene, the proposed method uses adaptive intra refresh rate with consideration of burst and guard locations. By locating the burst and guard sections, intra coded MBs are more guaranteed than the other methods. Thus, average PSNR of proposed method is higher.

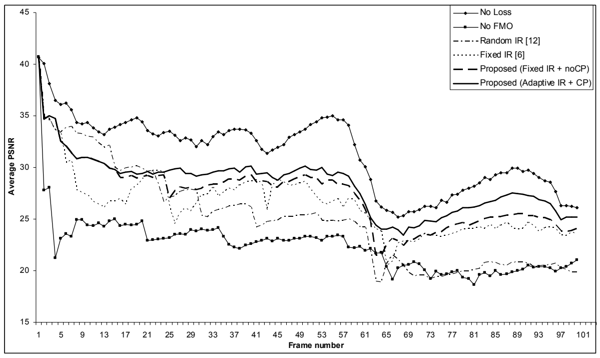

Fig.11 Average PSNR in slow fading

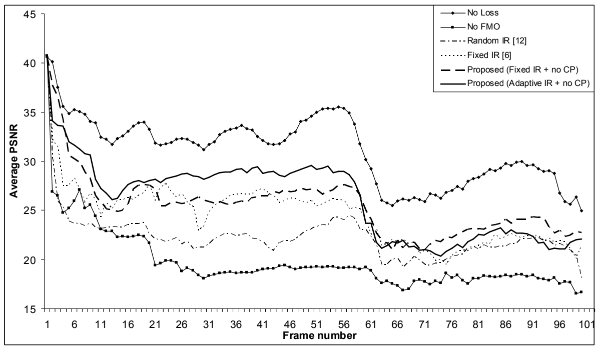

Fig. 12 Average PSNR in fast fading

Fig. 11 and Fig. 12 show the PSNR curve of methods using "Carphone" video sequence in slow and fast fading. In the slow fading case, because of channel prediction and adaptive intra refresh rate, the PSNR curve of the proposed method is higher than that of Random IR[13] and Fixed IR [8]. Since channel prediction is less precise in fast fading, average PSNR of "Adaptive IR +CP" is lower than "Fixed IR+ no CP" from frame 71 to frame 100. However, the results show in table 2 that the average PSNR of "Adaptive IR + CP" is still higher than the other methods.

To further illustrate improvement of the proposed method, some frames from the "Carphone" test sequence are extracted for comparison. Fig. 13, 14 and 15 depicts the subjective qualities of original 52nd frame of "Carphone" sequence and the reconstructed frames from four different methods including "Random IR", "Fixed IR", "Fixed IR + no CP" and "Adaptive IR + CP" in slow and fast fading. It can be seen that the subjective frame quality in "Random IR" is severely affected by error. However, in proposed method, this error can be substantially improved by using intra refresh and channel prediction.

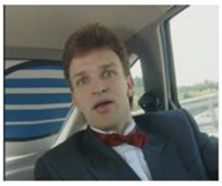

Fig. 13. Original frame 52nd

Fig. 14. Visual comparison of frame 52nd of "Carphone" sequence between methods in slow fading

Fig. 15. Visual comparison of frame 52nd of "Carphone" sequence between methods in fast fading

5. CONCLUSIONS

In this paper, based on estimating effect of error propagation, a FMO map is generated frame-by-frame. When considering inter-frame error propagation, intra refresh is also used and suitable intra refresh rate is selected based on the channel state to reduce the effect of error propagation. In addition, the three-state Markov model is used to estimate locations of burst and guard sections. With the predicted information of channel, important MBs are arranged into guard sections and less important MBs are arranged into burst sections. Experimental results show that our proposed method gains some improvements in terms of PSNR as compared to some other methods that have not taken channel condition and error propagation into consideration in generating FMO map.

6. ACKNOWLEDGMENTS

This research has been supported in part by the Collaborative Research Project entitled Wireless Video Transmission, JICA project for AUN/Seed-Net, Japan.

7. REFERENCES

1. *ITU-T Recommendation H.264: "Advance video coding for generic audiovisual", March 2005.*

2. *W. Hanatanong, and S. Aramvith, " Analysis of macrobloc-to-slice group mapping for H.264 Video Transmission over Packet-Based Wireless Fading Channel", 48th Midwest Symposium on Ctkt and Sys., vol.2, pp. 1541-1544, August 2005.*

3. *J. Panyavaraporn, R. Cajote, and S. Aramvith, "Performance Analysis of Flexible Macroblock Ordering using Bitcount and Distortion measure for H.264 Wireless Video Transmission", International Workshop on Smart Info-Media Systems in Bangkok (SISB 2007), Bangkok, Thailand, Nov. 2007.*

4. *Y. Dhont, P. Lambert, and R. Van der Walle, "A Flexible macroblock scheme for unequal error protection", ICIP 2006.*

5. *R. D. Cajote, S. Aramvith, R.C.L. Guevara, and Y. Miyanaga, "FMO slice group maps using spatial and temporal indicators for H.264 wireless video transmission", Circuits and Systems, ISCAS 2008, pp. 3566-3569, May. 2008.*

6. *J.Y. Shih, and W.J. Tsai, "A new unequal error protection scheme based on FMO", ICIP 2008, 15th IEEE Int'l Conference, pp. 3068-3071, Oct. 2008.*

7. *B. Katz, S. Greenberg, N. Yarkoni, N. Blaunstien, and R. Giladi, "New error-resilient scheme based on FMO and Dynamic Redundant slices allocation for wireless video transmission", IEEE Trans., vol. 53, no. 1, pp. 308-319, march 2007.*

8. *B. Girod, and N. Farber, "Error-resilient standard compliant video coding", available at link: http://citeseerx.ist.psu.edu/viewdoc/summary?doi=10.1.1.51.6841.*

9. *P. Nunes, L.D. Soares, and F. Pereira, "Error resilience macroblock rate control for H.264/AVC video coding", ICIP 2008, 15th IEEE Int'l Conference, pp. 2132-2135.*

10. *Jin Xu, and Zhimei Wu, "Joint adaptive intra refreshment and unequally error protection algorithms for robust transmission of H.264/AVC video", Multimedia and Expo, 2006, IEEE Int'l Conference, pp. 693-696, July 2006.*

11. *T. Sato, K. Tokuda, M. Kawabe, and T. Kato, "Simulation of burst error models and adaptive error control scheme for high speed data transmission over analog cellular system", IEEE Trans. Veh. Technol., vol. VT-40, pp. 443-453, May 1991.*

12. *T. Sata, M. Kawabe, T. Kato, and A. Fukasawa, "Throughput analysis method for hybrid ARQ schemes over bust error channels", IEEE Trans. Veh. Technol., vol. 40, no. 1, pp. 110-118, Feb 1993.*

13. *Michael, K. K. Sühring, and G. Sullivan, "Proposed H.264/MPEG-4 AVC Reference Sofware Manual", Joint Video Team, Doc. JVTM012, Palma(Spain), Oct. 2004.*

14. *T.C. Chen, et al., "A real-time software based end-to-end wireless visual communications simulation platform", Proc. SPIE Visual Comms. and Image Processing, vol. 3, pp. 1068-1074, May 1995.*

15. *Institute of Computing Technology, "Proposed Draft of Adaptive Rate Control", Joint Video Team(JVT), doc. JVT-H014, 8th meeting Geneva, May 20-26, 2003.*

Vu Huu Tien

He received B. Eng. and M.S degrees in electrical engineering from Hanoi University of Technology, Hanoi, Vietnam in 2002 and 2004, respectively. He received Ph.D. degrees in electrical engineering from Chulalongkorn University, Thailand, in 2011. He is currently a researcher in Posts and Telecommunications Institute of Technology, Hanoi, Vietnam. His research interests are in the area of error resilient for video coding, cross-layer wireless multimedia.

Supavade Aramvith

She received the B.S. (first class honors) degree in computer science from Mahidol University, Bangkok, Thailand, in 1993. She received the M.S. and Ph.D. degrees in electrical engineering from the University of Washington, Seattle, USA, in 1996 and 2001, respectively.

She is currently an Assistant Professor at Department of Electrical Engineering, Chulalongkorn University, Bangkok, Thailand. She is IEEE Senior member and also serves as IEEE Thailand Section Secretary and Conference manager and Executive secretary of IEICE Bangkok area representative. Her research interests include video object segmentation, detection, and tracking, rate-control for video coding, joint source-channel. coding for wireless video transmissions, and image/video retrieval techniques.

Yoshikazu Myanaga

He received his B. Eng., ME., and D. Eng. Degrees from Hokkaido Univeristy, Sapporo Japan, in 1979, 1981, and 1986, respectively. He is currently a Professor in the laboratory for Information Communication Networks, Division of Media and Network Technoloty at the Graduate School of Information Science and Technology, Hokkaido University.

His research interests are in the areas of adaptive signal processing and parallel/pipelined VLSI system.